



ELSEVIER

Contents lists available at ScienceDirect

## Data in Brief

journal homepage: [www.elsevier.com/locate/dib](http://www.elsevier.com/locate/dib)

## Data Article

# TCA precipitation and ethanol/HCl single-step purification evaluation: One-dimensional gel electrophoresis, Bradford assays, spectrofluorometry and Raman spectroscopy data on HSA, Rnase, lysozyme - Mascots and Skyline data



Balkis Eddhif<sup>a</sup>, Nadia Guignard<sup>b</sup>, Yann Batonneau<sup>b</sup>,  
Jonathan Clarhaut<sup>c,d</sup>, Sébastien Papot<sup>c</sup>,  
Claude Geffroy-Rodier<sup>a</sup>, Pauline Poinot<sup>a,\*</sup>

<sup>a</sup> Institut de Chimie des Milieux et des Matériaux de Poitiers (IC2MP), Université de Poitiers, CNRS, Equipe Eaux, Biomarqueurs, Contaminants Organiques, Milieux, (E-BiCOM), 4 rue Michel Brunet, TSA 51106, F-86073 Poitiers, France

<sup>b</sup> Institut de Chimie des Milieux et des Matériaux de Poitiers (IC2MP), Université de Poitiers, CNRS, Equipe Site Actif au Matériau Catalytique (SAMCat), 4 rue Michel Brunet, TSA 51106, F-86073 Poitiers, France

<sup>c</sup> Institut de Chimie des Milieux et des Matériaux de Poitiers (IC2MP), Université de Poitiers, CNRS, Equipe Synthèse Organique, 4 rue Michel Brunet, TSA 51106, F-86073 Poitiers, France

<sup>d</sup> CHU de Poitiers, 2 rue de la Miléterie, CS 90577, F-86021 Poitiers, France

## ARTICLE INFO

## Article history:

Received 24 November 2017

Accepted 30 January 2018

Available online 5 February 2018

## ABSTRACT

The data presented here are related to the research paper entitled “Study of a Novel Agent for TCA Precipitated Proteins Washing - Comprehensive Insights into the Role of Ethanol/HCl on Molten Globule State by Multi-Spectroscopic Analyses” (Eddhif et al., submitted for publication) [1]. The suitability of ethanol/HCl for the washing of TCA-precipitated proteins was first investigated on standard solution of HSA, cellulase, ribonuclease and lysozyme. Recoveries were assessed by one-dimensional gel electrophoresis, Bradford assays and UPLC-HRMS. The mechanistic that triggers protein conformational changes at each purification stage was then investigated by Raman spectroscopy and spectrofluorometry.

DOI of original article: <https://doi.org/10.1016/j.jprot.2017.11.016>

\* corresponding author.

E-mail address: [pauline.poinot@univ-poitiers.fr](mailto:pauline.poinot@univ-poitiers.fr) (P. Poinot).

<https://doi.org/10.1016/j.dib.2018.01.095>

2352-3409/© 2018 The Authors. Published by Elsevier Inc. This is an open access article under the CC BY license (<http://creativecommons.org/licenses/by/4.0/>).

Finally, the efficiency of the method was evaluated on three different complex samples (mouse liver, river biofilm, loamy soil surface). Proteins profiling was assessed by gel electrophoresis and by UPLC-HRMS.

© 2018 The Authors. Published by Elsevier Inc. This is an open access article under the CC BY license (<http://creativecommons.org/licenses/by/4.0/>).

## Specifications Table

Subject area	Chemistry
More specific subject area	Proteomics, protein purification, protein precipitation, trichloroacetic acid
Type of data	Tables, Figures
How data was acquired	Raman (LabRAM HR800UV confocal microspectrometer, Horiba Jobin Yvon, Kyoto, Japan) Bradford assay (DC Protein Assay, Biorad) Electrophoresis (ImageJ software) UPLC-HRMS (Accela LC pumps, Q-Exactive Hybrid Quadrupole-Orbitrap mass spectrometer equipped of an ESI source, Thermo Fisher Scientific, Waltham, MA, USA) MASCOT search engine (Matrix Science, London, UK; version 2.6.0) and Skyline software (MacCoss Lab, Washington, US; version 3.7.0.10940) ProteomeXchange Consortium with identifier PXD008110
Data format	Raw, analyzed and processed data
Experimental factors	
Experimental features	Proteins extraction was performed on 500 mg of soil, 10 mg of biofilm and 15 mg of mouse liver as starting material according to protocols of Chourey et al. [2], Huang et al. [3] and Song et al. [4] respectively. Proteins were precipitated with 25% (w/v) trichloroacetic acid (TCA). The washing of protein pellet was performed with three different agents (acetone, ethanol, or ethanol/HCl). The mixture was vortexed and kept at $-20^{\circ}\text{C}$ for 1 h, centrifuged at 16,600 g for 15 min at $4^{\circ}\text{C}$ . The resulting pellets were dried in a SpeedVac concentrator, solubilized in a 50 mM of ammonium bicarbonate buffer containing 10 mM of Tris. Proteins were subjected to trypsin digestion for 24 h at $37^{\circ}\text{C}$ . Digestion was stopped with formic acid before gel, bradford and mass analysis.
Data source location	Poitiers, France
Data accessibility	data are with this article

## Value of the data

- Data show a comprehensive evaluation of protein conformational changes throughout TCA precipitation and one single step purification with various solvents.
- Data highlight the efficiency of ethanol/HCl purification for TCA-precipitated proteins.
- Ethanol/HCl represents a quick and inexpensive purification agent for proteomics studies.
- Presence and variability of proteins are potential values to determine which purification method must be used for proteomics investigation.

## 1. Data

TCA precipitation is one of the most common and robust technique required for protein analyses [5–7]. However it leads to molten globule states which hamper the solubilization of proteins in aqueous buffers for mass spectrometry analysis.

### 1.1. Comparison of washing agents on standard solutions

A standard solution of HSA, cellulase (exoglucanases and endoglucanases mixture), lysozyme and ribonuclease A,  $35 \mu\text{g mL}^{-1}$  each, was prepared in high purified water. Proteins were precipitated with 25% (w/v) trichloroacetic acid (TCA) (final concentration). The clean-up of protein pellet was performed following three different approaches: ethanol/HCl (1.25 M; 3.8%), acetone/HCl (0.06 M; 0.2%); acetone/HCl (1.25 M; 3.8%) (Fig. 1).

### 1.2. Extraction and purification of endogenous proteins from complex sample matrices

See Fig. 2.

### 1.3. Effects of successive ethanol/HCl washings on proteins recoveries

10 mg of biofilm samples were spiked with the standard solution of HSA, exoglucanase 1 from the mix of cellulase, lysozyme, and ribonuclease A (Rnase). Proteins final concentration was  $1 \mu\text{g mg}^{-1}$  of matrix to enable HRMS detection of the proteins after the whole process. The mixture was vortexed and left during 24 h at room temperature to favor proteins adsorption on the matrix. After extraction following the published protocol of Huang et al. [3], protein pellets were subjected to one, two or three ethanol/HCl washing(s).

They were then dissolved in 50 mM of ammonium bicarbonate containing 10 mM of Tris (pH 8.5), diluted in a ratio of 1:3 using the same buffer and subjected to trypsin digestion.

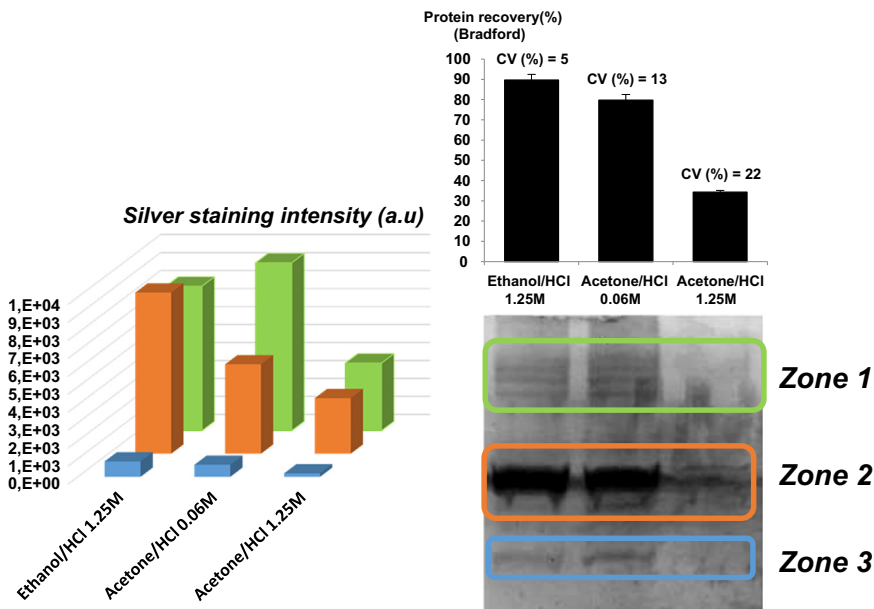


**Fig. 1.** Standard proteins quantification by Bradford assay and silver-staining on electrophoresis gel. The thin line bars represent standard deviations at the top of the Bradford histogram. For both methods, histograms were constructed from the mean value of three independent assays.

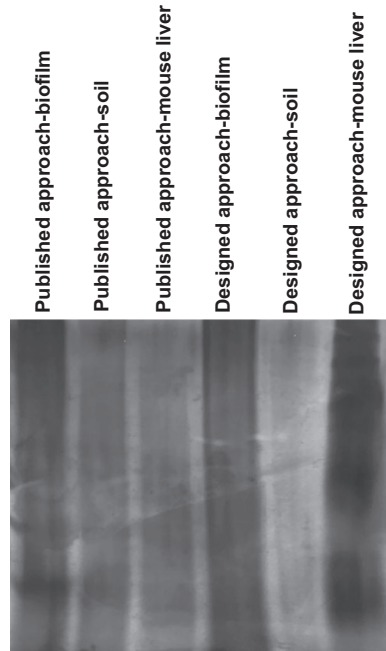


**Fig. 2.** One-dimensional gel electrophoresis of complex matrices (biofilm, soil and mouse liver) after purification following the designed approach versus published protocols on complex matrices. The gel was stained with silver nitrate.

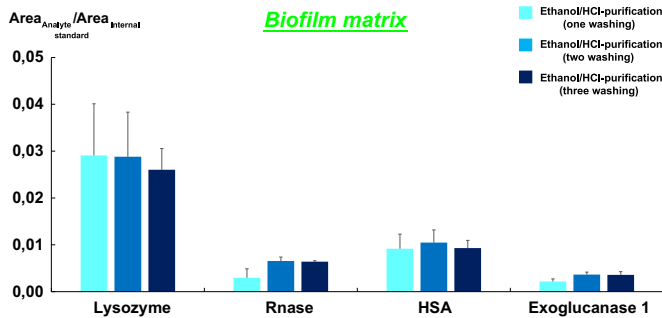


**Fig. 3.** Proteins recoveries following the designed approach on biofilm sample. The thin line bars represent standard deviations at the top of each column. Each bar shows mean  $\pm$  s.e.m. from three independent purification assays. Protein recoveries in Tris buffer were determined by UPLC/HRMS in a full scan mode with a resolution of 70.000 and mass range of 200–3000 m/z.

Experiments were performed in triplicate. Fig. 3 gives the mean protein recoveries following the designed approach (Ethanol/HCl) on biofilm matrix after multiple washing steps.

#### 1.4. Understanding the effect of ethanol/HCl on proteins conformation

##### 1.4.1. Spectrofluorometry

To get insights into the role of ethanol/HCl on proteins solubility, their conformational changes were comprehensively investigated, as an extension of the results reported in Ref. [1]. These measures were performed at each purification stage with two spectroscopic techniques: spectrofluorometry and Raman.

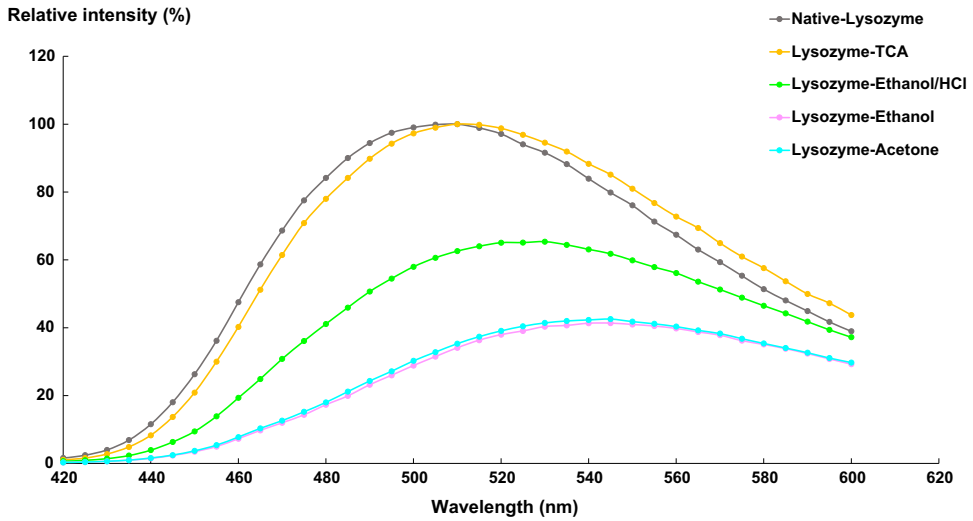


**Fig. 4.** Emission spectra of lysozyme ( $\lambda_{exc} = 400$  nm) at different purification steps. Native lysozyme (grey spectrum); Lysozyme-TCA (orange spectrum); Lysozyme-ethanol/HCl (green spectrum); Lysozyme-ethanol (purple spectrum); Lysozyme-acetone (blue spectrum).

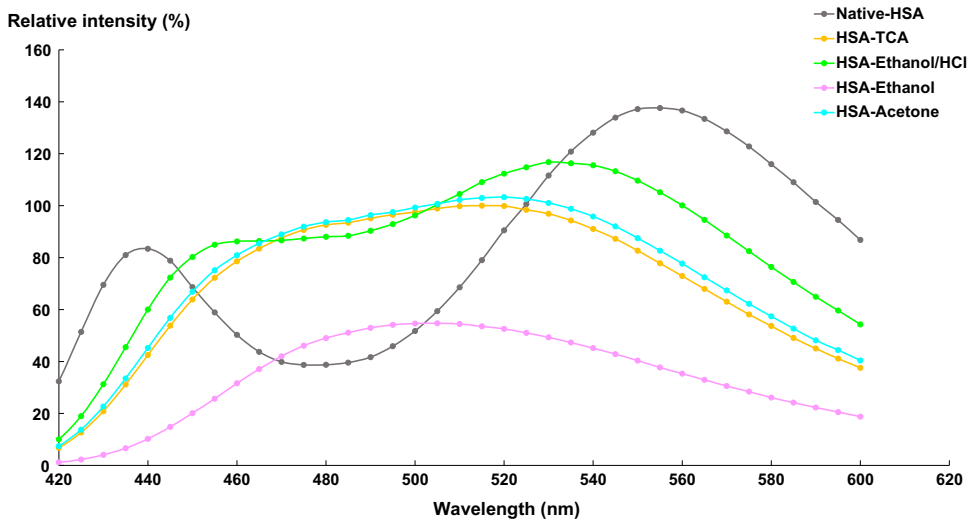


**Fig. 5.** Emission spectra of HSA ( $\lambda_{exc} = 400$  nm) at different purification steps. Native HSA (grey spectrum); HSA-TCA (orange spectrum); HSA-ethanol/HCl (green spectrum); HSA-ethanol (purple spectrum); HSA-acetone (blue spectrum).

Figs. 4–6 represent the fluorescence emission spectra of lysozyme, HSA and Rnase after TCA precipitation and washing steps (ethanol/HCl, ethanol or acetone).

#### 1.4.2. Raman microspectroscopy

Raman spectrum for Rnase, is presented in Fig. 7. Spectra and curve fitting of the amide I band of proteins corresponding to lysozyme and HSA are presented in Figs. 5 and 6 in Ref. [1], respectively (Figs. 8–11).

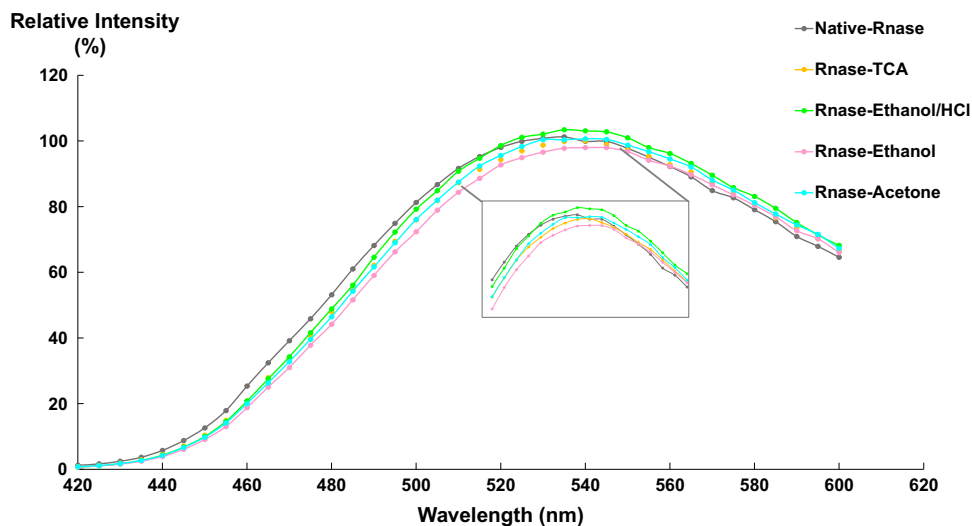


**Fig. 6.** Emission spectra of RNase ( $\lambda_{exc} = 400$  nm) at different purification steps. Native Rnase (grey spectrum); Rnase-TCA (orange spectrum); Rnase-ethanol/HCl (green spectrum); Rnase-ethanol (purple spectrum); Rnase-acetone (blue spectrum).

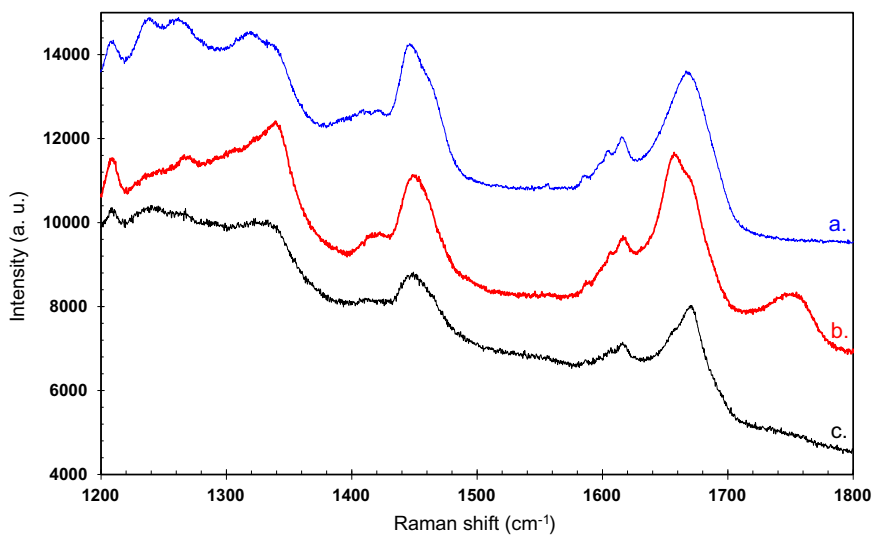


**Fig. 7.** Raman spectra of RNase at different purification steps (range 1200–1800  $\text{cm}^{-1}$ ). a. Native Rnase (blue spectrum); b. Rnase-TCA (red spectrum) (shifted 1500 arbitrary units (a. u.) downward); c. Rnase-ethanol/HCl (black spectrum) (shifted 600 a. u. upward).

The unfolding or aggregation of proteins usually involves some dynamic changes in their secondary structures. These changes are mainly monitored by the analysis of the amide I region (1600–1690  $\text{cm}^{-1}$ ) which is assumed to be sensitive to  $\alpha$ -helical secondary structures [8].

### 1.5. Extraction and purification of proteins from complex samples: LC-HRMS analysis

We present processed data of UPLC- HRMS analysis of proteins from different samples (mouse liver, river biofilm, soil) after TCA precipitation and solvent purification. The datasets in XML format

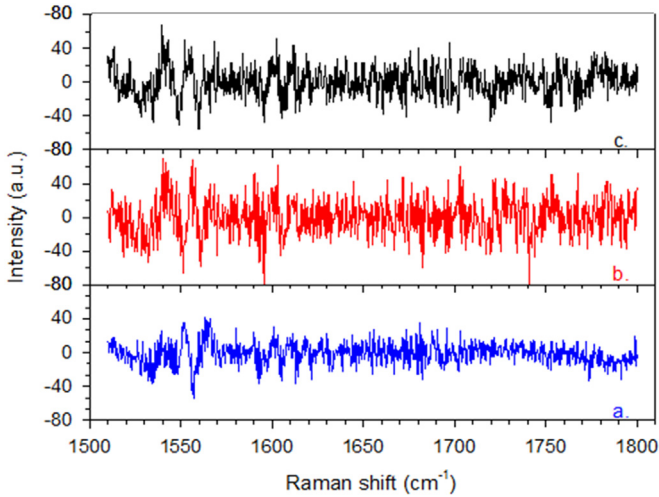


**Fig. 8.** Difference spectra (experimental – fitting curve) after analysis of the amide I Raman bands of lysozyme at different purification steps (Fig. 5, [1]). a. Native lysozyme (blue); b. Lysozyme-TCA (red); c. Lysozyme-ethanol/HCl (black).

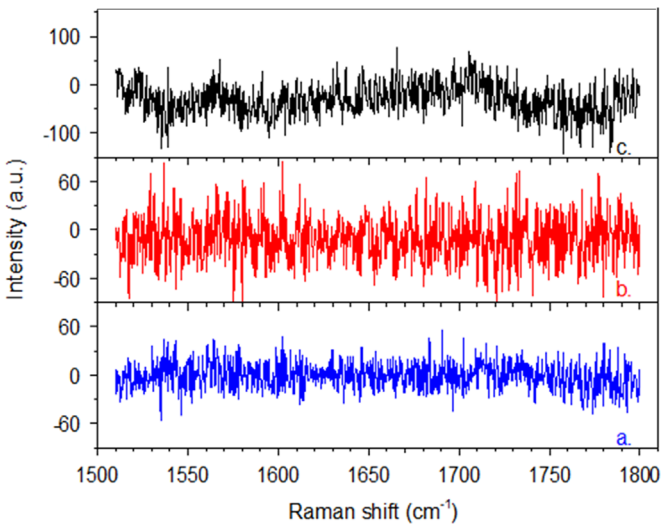


**Fig. 9.** Difference spectra (experimental – fitting curve) after analysis of the amide I Raman bands of HSA at different purification steps (Fig. 6, [1]). a. Native HSA (blue); b. HSA-TCA (red); c. HSA-ethanol/HCl (black).

can be used to evaluate ethanol/HCl purification for proteins profiling. Table 1 gives the HRMS features of peptides targeted for the standard proteins after *in silico* tryptic digestion. Table 2 presents endogenous proteins identified in soil, biofilm and mouse liver samples after purification following either the designed approach or published protocols (Mascot identification). Table 3 presents endogenous proteins detected in the mouse liver sample and quantified through Skyline with corresponding peptides and transitions for PRM. Table 4 presents endogenous proteins detected in the biofilm sample and quantified through Skyline with corresponding peptides and transitions for PRM (Table 5).

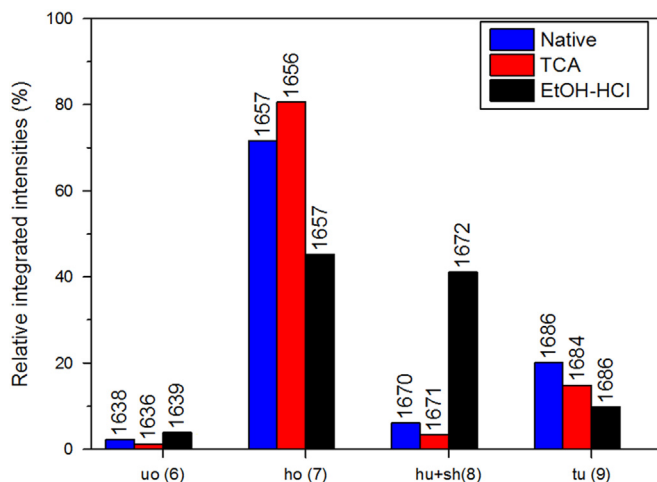


**Fig. 10.** Relative integrated intensities of lysozyme amide I contribution from peak #6 assigned to unordered structures (*uo*), peak#7 (ordered  $\alpha$  helices, *ho*), peak#8 (unordered  $\alpha$  helices and  $\beta$  sheets, *hu+sh*), and peak #9 (turns, *tu*) as obtained after profile fitting of amide I region of the Raman spectra (Fig. 5, Ref. [1]). Values on top of each bar correspond to the Raman shift on which the contribution peak was centred at the end of the fitting.

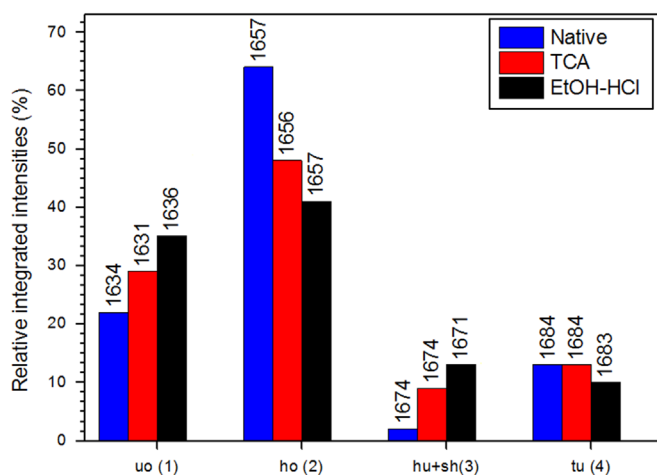


**Fig. 11.** Relative integrated intensities of HSA amide I contribution from peak #1 assigned to unordered structures (*uo*), peak#2 (ordered  $\alpha$  helices, *ho*), peak#3 (unordered  $\alpha$  helices and  $\beta$  sheets, *hu+sh*), and peak #4 (turns, *tu*) as obtained after profile fitting of amide I region of the Raman spectra shown in Fig. 6 [1]. Values on top of each bar correspond to the Raman shift on which the contribution peak was centred at the end of the fitting.

**Table 1**

HRMS features of peptides targeted for the four standard proteins after in silico tryptic digestion.

Protein name	Peptide sequence	[M+H] <sup>1+</sup>	[M+2H] <sup>2+</sup>	[M+3H] <sup>3+</sup>	[M+4H] <sup>4+</sup>
LYSO-1	FESNFNTQATNR		714.8288	476.8883	
LYSO-2	HGLDNYR	874.4166	437.7119	292.1437	
RNASE-1	CKPVNTFVHESLADVQAVCS QK			839.7457	630.0611
RNASE-2	HIIVACEGNPYVPVHFDASV		1112.5464	742.0334	
RNASE-3	YPNCAYK	915.4029	458.2051		
HSA-1	AVMDDFAAFVEK		671.8210	448.2164	
HSA-2	LVAASQAALGL	1013.5990	507.3031		
HSA-3	YLYEIAK	927.4934	464.2504	309.8360	
EXO-1	GSCSTSSGVPAQVESQSPNA K		1039.4764	693.3200	
EXO-2	YGTGYCDSQCPR		732.2876	488.5275	
EXO-3	VTFSNIK	808.4563	404.7282		



**Table 2**

Endogenous proteins identified in soil, biofilm and mouse liver after purification following either the designed approach or the published protocols.

Sample	Location	Protein name	Phylogenetic origin	Protein coverage (%)		Score <sup>a</sup>		GRAVY	MW (Da) <sup>b</sup>
				The designed approach	Published protocol	The designed approach	Published protocol		
Soil	Extracellular region	Endoglucanase EG-II	<i>Hypocrea jecorina</i>	18	19	161	251	-0.19	44883
	Extracellular region	Xyloglucanase	<i>Hypocrea jecorina</i>	1	1	76	114	-0.21	87307
Biofilm	Cellular thylakoid membrane ; Peripheral membrane protein ; Cytoplasmic side	<b>C-phycoerythrin alpha chain</b>	<b><i>Microchaete diplosiphon</i></b>	<b>29</b>	<b>29</b>	<b>269</b>	<b>239</b>	-0.15	<b>17786</b>
		<b>R-phycoerythrin alpha chain</b>	<b><i>Porphyra purpurea</i></b>	<b>20</b>	<b>17</b>	<b>168</b>	<b>119</b>	-0.19	<b>17972</b>
	chloroplast thylakoid membrane ; Peripheral membrane protein By similarity; Stromal side	<b>C-phycoerythrin alpha chain</b>	<b><i>Synechococcus sp.</i></b>	<b>17</b>	<b>17</b>	<b>181</b>	<b>177</b>	-0.11	<b>17335</b>
		<b>C-phycoerythrin alpha chain</b>	<b><i>Synechocystis sp.</i></b>	<b>20</b>	<b>20</b>	<b>209</b>	<b>176</b>	-0.12	<b>17756</b>
	Cellular thylakoid membrane; Peripheral membrane protein ; Cytoplasmic side	Allophycocyanin alpha chain 1	<i>Microchaete diplosiphon</i>	11	11	76	84	-0.14	17411
	Cellular thylakoid membrane ; Peripheral membrane protein ; Cytoplasmic side	B-phycoerythrin beta chain	<i>Porphyridium purpureum</i>	21	20	117	183	0.25	18884
	Cellular thylakoid membrane ; Peripheral membrane protein ; Cytoplasmic side	C-phycoerythrin beta chain	<i>Microchaete diplosiphon</i>	21	16	138	85	0.21	19568
	chloroplast thylakoid membrane ; Peripheral membrane protein ; Stromal side	R-phycoerythrin beta chain	<i>Pyropia haitanensis</i>	23	28	129	144	0.26	18810
	Cellular thylakoid membrane ; Peripheral membrane protein ; Cytoplasmic side	C-phycoerythrin alpha chain	<i>Microchaete diplosiphon</i>	16	12	64	122	0.17	18080
	Cellular thylakoid membrane ; Peripheral membrane protein ; Cytoplasmic side	Allophycocyanin subunit alpha 1	<i>Nostoc sp.</i>	17	19	99	112	-0.09	17392
	chloroplast thylakoid membrane ; Peripheral membrane protein ; Stromal side	C-phycoerythrin beta chain	<i>Aglaothamnion neglectum</i>	11	12	112	111	0.09	18290
	NI	Ribulose biphosphate carboxylase large chain	<i>Trichodesmium erythraeum</i>	5	8	90	122	-0.32	53615
	Cellular thylakoid membrane ; Peripheral membrane protein ; Cytoplasmic side	Allophycocyanin alpha chain	<i>Anabaena cylindrica</i>	6	11	84	83	0.01	17128
	Cellular thylakoid membrane ; Peripheral membrane protein ; Cytoplasmic side	C-phycoerythrin alpha chain	<i>Pseudanabaena tenuis</i>	18	18	144	126	-0.24	17780
chloroplast thylakoid membrane ; Multi-pass membrane protein	Photosystem II CP47 reaction center protein	<i>Odontella sinensis</i>	8	8	117	114	0.08	56436	

	NI	Ribulose biphosphate carboxylase large chain	<i>Cyanothece sp.</i>	9	6	94	89	-0.27	53531
	chloroplast	Ribulose biphosphate carboxylase large chain (Fragment)	<i>Calyptrosphaera sphaeroidea</i>	5	9	90	107	-0.10	50919
	chloroplast	Ribulose biphosphate carboxylase large chain	<i>Gracilaria tenuistipitata var. liui</i>	8	10	111	132	-0.10	54442
	chloroplast	Ribulose biphosphate carboxylase large chain	<i>Cylindrotheca sp.</i>	6	6	109	108	-0.12	54400
	chloroplast thylakoid membrane ; Peripheral membrane protein ; Stromal side chloroplast	Allophycocyanin beta chain	<i>Cyanidium caldarium</i>	13	16	94	83	-0.04	17574
		Ribulose biphosphate carboxylase small chain	<i>Antithamnion sp.</i>	5	5	72	72	-0.58	16247
	NI	Carbon dioxide-concentrating mechanism protein CcmK homolog 1	<i>Synechocystis sp.</i>	18	29	71	72	-0.19	11128
	chloroplast thylakoid membrane ; Peripheral membrane protein ; Stromal side chloroplast	R-phycoerythrin beta chain	<i>Aglaothamnion neglectum</i>	7	7	100	69	0.27	18710
		Ribulose biphosphate carboxylase large chain (Fragment)	<i>Haptolina hirta</i>	9	10	141	139	-0.11	51098
	chloroplast	Ribulose biphosphate carboxylase large chain	<i>Antithamnion sp.</i>	7	7	117	113	-0.12	54372
	Cellular thylakoid membrane ; Peripheral membrane protein ; Cytoplasmic side	Allophycocyanin beta chain	<i>Thermosynechococcus elongatus</i>	18	18	103	121	0.10	17462
	Cell inner membrane ; Multi-pass membrane protein	Photosystem I P700 chlorophyll a apoprotein A2	<i>Gloeobacter violaceus</i>	2	2	78	75	0.15	96126
	chloroplast thylakoid membrane; Peripheral membrane protein; Stromal side	Phycobiliprotein ApcE	<i>Aglaothamnion neglectum</i>	1	1	73	72	-0.23	101319
	NI	Ribulose biphosphate carboxylase large chain	<i>Synechocystis sp.</i>	6	6	120	117	-0.29	53084
	chloroplast thylakoid membrane; Peripheral membrane protein; Stromal side	Allophycocyanin beta chain	<i>Galdieria sulphuraria</i>	16	16	96	73	0.02	17536
Mouse liver	Nucleus, Mitochondrion	<b>Carbamoyl-phosphate synthase</b>	<b><i>Mus musculus</i></b>	<b>39</b>	<b>33</b>	<b>1637</b>	<b>1268</b>	-0.12	<b>165711</b>
	Cytoplasm	<b>Arginase-1</b>	<b><i>Mus musculus</i></b>	<b>29</b>	<b>35</b>	<b>300</b>	<b>310</b>	-0.19	<b>34957</b>
	Cytosol, Nucleus, Membrane	<b>Selenium-binding protein</b>	<b><i>Mus musculus</i></b>	<b>31</b>	<b>28</b>	<b>526</b>	<b>405</b>	-0.31	<b>53147</b>
	Cytoplasm	<b>Argininosuccinate synthase</b>	<b><i>Mus musculus</i></b>	<b>32</b>	<b>15</b>	<b>429</b>	<b>191</b>	-0.11	<b>46840</b>
	Mitochondrion	<b>Glyceraldehyde-3-phosphate dehydrogenase</b>	<b><i>Mus musculus</i></b>	<b>31</b>	<b>32</b>	<b>321</b>	<b>298</b>	-0.04	<b>36072</b>
	cytosol	Cytosolic 10-formyltetrahydrofolate dehydrogenase	<i>Mus musculus</i>	9	17	139	361	-0.36	99502
	Extracellular region	3-ketoacyl-CoA thiolase, mitochondrial	<i>Mus musculus</i>	10	20	137	216	-0.38	42260

Table 2 (continued)

Sample	Location	Protein name	Phylogenetic origin	Protein coverage (%)		Score <sup>a</sup>		GRAVY	MW (Da) <sup>b</sup>
				The designed approach	Published protocol	The designed approach	Published protocol		
	Nucleus, Cytoskeleton, Cytosol	Serum albumin	<i>Mus musculus</i>	15	18	327	349	-0.09	70700
	Cytoplasm	Alcohol dehydrogenase 1	<i>Mus musculus</i>	19	29	161	212	0.20	40601
	membrane	Aspartate aminotransferase, mitochondrial	<i>Mus musculus</i>	15	16	231	215	-0.23	47780
	Endoplasmic reticulum	Carboxylesterase 3B	<i>Mus musculus</i>	12	14	201	183	-0.12	63712
	Cytoplasm	Glycine N-methyltransferase	<i>Mus musculus</i>	29	19	131	127	-0.25	33110
	membrane	Cytochrome P450 2D10	<i>Mus musculus</i>	9	2	100	123	-0.06	57539
	Cytoplasm	Aspartate aminotransferase, cytoplasmic	<i>Mus musculus</i>	7	13	112	115	-0.25	46504
	Cytoplasm	Adenosylhomocysteinase	<i>Mus musculus</i>	27	14	335	120	-0.07	47780
	Cytosol	Fructose-1,6-bisphosphatase 1	<i>Mus musculus</i>	12	16	117	120	-0.12	37288
	Endoplasmic reticulum	Carboxylesterase 3A	<i>Mus musculus</i>	13	9	220	139	-0.12	63677
	Mitochondrion	Sarcosine dehydrogenase, mitochondrial	<i>Mus musculus</i>	8	6	182	209	-0.25	102644
	membrane	UDP-glucuronosyltransferase 1-1	<i>Mus musculus</i>	4	8	94	141	0.09	60749
	Cytosol	Hemoglobin subunit beta-1	<i>Mus musculus</i>	16	24	111	105	0.08	15944
	Peroxisome	Peroxisomal bifunctional enzyme	<i>Mus musculus</i>	3	2	98	78	-0.12	78822
	membrane	Microsomal glutathione S-transferase	<i>Mus musculus</i>	17	21	80	87	0.15	17597
	membrane	Cytochrome P450 2F2	<i>Mus musculus</i>	6	7	128	130	-0.13	56141
	NI	Pyrethroid hydrolase Ces2a	<i>Mus musculus</i>	9	5	100	76	-	57539
	Extracellular region	Homogentisate 1,2-dioxygenase	<i>Mus musculus</i>	6	6	81	114	-0.34	50726
	Cytoplasm	Regucalcin	<i>Mus musculus</i>	4	13	72	112	-0.28	33899
	Peroxisome	3-ketoacyl-CoA thiolase B, peroxisomal	<i>Mus musculus</i>	13	8	116	84	0.05	44481
	membrane	Sorbitol dehydrogenase	<i>Mus musculus</i>	6	6	90	89	0.06	38795
	membrane	ATP synthase subunit f, mitochondrial	<i>Mus musculus</i>	26	26	70	71	-0.30	10394
	membrane	ATP synthase subunit alpha, mitochondrial	<i>Mus musculus</i>	14	10	193	160	-0.10	59830
	Cytosol	Urocanate hydratase	<i>Mus musculus</i>	2	1	100	76	-0.14	75227
	Extracellular region	Fumarylacetoacetase	<i>Mus musculus</i>	3	6	75	74	-0.21	46488
	Mitochondrion; Peroxisome	Uricase	<i>Mus musculus</i>	17	11	157	97	-0.46	35245
	Cytoskeleton		<i>Mus musculus</i>	15	13	180	119	-0.26	39938

	Fructose-bisphosphate aldolase B								
membrane	UDP-glucuronosyltransferase 2B17	<i>Mus musculus</i>	11	6	104	96	-0.03	61386	
NI	Pyrethroid hydrolase	<i>Mus musculus</i>	9	7	108	89	-0.08	62356	
Cytoplasm	3-hydroxyanthranilate 3,4-dioxygenase	<i>Mus musculus</i>	9	6	90	87	-0.55	32955	
Mitochondrion	Hydroxymethylglutaryl-CoA synthase, mitochondrial	<i>Mus musculus</i>	7	6	86	70	-0.34	57300	
Mitochondrion	Trifunctional enzyme subunit alpha, mitochondrial	<i>Mus musculus</i>	9	7	90	81	-0.10	83302	
Endoplasmic reticulum	Microsomal triglyceride transfer protein large subunit	<i>Mus musculus</i>	1	1	74	80	-0.16	99664	
membrane	Cytochrome b-c1 complex subunit 2, mitochondrial	<i>Mus musculus</i>	4	4	73	76	-0.06	48262	

<sup>a</sup> MASCOT score greater than 67.

<sup>b</sup> MW: Molecular weight.

**Table 3**  
Endogenous peptides and transitions for PRM methods.

Protein name	Abreviattion	Peptide	PRM	
			Precursor( <i>m/z</i> )	Product ( <i>m/z</i> )
Carbamoyl-phosphate synthase	CPSM	TAVDSGIALLTNFQVTK	898.4844	950.5306
				837.4465
		VLGTSVESIMATEDR	804.4009	736.3988
				1051.4725
				722.3138
		AFAMTNQILVER	696.8688	591.2733
				972.5473
		GQNQPVLNITNR	677.3653	516.3140
				403.2300
		AADTIGYPVMIR	653.8448	926.5418
617.3365				
EPLFGISTGNIITGLAAGAK	644.0263	390.2096		
		835.4495		
		615.3647		
		472.2402		
		801.4829		
IALGIPLPEIK	582.3735	688.3988		
		587.3511		
VMIGESIDEK	560.7814	696.4291		
		355.2340		
SVGEVMAIGR	509.7711	468.3180		
		890.4466		
		777.3625		
Argininosuccinate synthase	ASSY	EQGYDVIAYLANIGQK	891.4571	231.1162
				832.4345
		FELTCYSLAPQIK	785.4027	646.3705
				547.3021
		QHGIPIVTPK	593.8508	977.5415
				743.4410
		NQAPPGLYTK	544.7904	630.3570
				1085.4972
		YLLGTSLARPCIAR	530.9643	556.3453
				485.3082
Selenium-binding protein 2	SBP2	GSFVLLDGETFEVK	770.8983	921.5768
				751.4713
		EIVYLPCIYR	727.871	541.3344
				846.472
		LTGQIFLGGSSIVR	680.901	775.4349
				314.1459
		IYVVDVGSEPR	617.3273	657.8692
				601.3271
IFVWDWQR	575.2956	277.1547		
		1037.515		
VIEASEIQAK	544.3033	924.4309		
		809.404		
		984.4971		
		821.4338		
		708.3498		
		848.4989		
		701.4304		
		588.3464		
		957.5		
		858.4316		
		545.2678		
		889.4315		
		790.3631		
		261.1598		
		875.4469		
		746.4043		

**Table 3** (continued)

Protein name	Abreviattion	Peptide	PRM	
			Precursor(m/z)	Product (m/z)
				675.3672
Glyceraldehyde-3-phosphate dehydrogenase	G3P	VPTPNVSVDLTCR	778.9087	1259.6412 949.4771
		WGEGAGAEYVVESTGVFTTMEK	764.3561	630.3243 912.4495 892.4123
		GAAQNIIPASTGAAK	685.3753	756.3597 815.4621 702.3781
		LISWYDNEYGYSNR	593.9373	668.3726 1021.4625 539.2572 376.1939
Arginase-1	ARGI1	VMEETFSYLLGR	722.8607	1214.6052 855.4723 708.4039
		EGLYITEEIIYK	679.3479	1058.5405 895.4771 782.3931
		VSVVLGGDHSLAVGSISGHAR	673.3641	866.9581 817.4239 760.8819
		SLEIIGAPFSK	581.3293	606.3246 556.3341 478.266

**Table 4**  
Endogenous peptides and transitions for PRM methods.

Protein name	Abreviattion	Peptide	PRM	
			Precursor(m/z)	Product (m/z)
R-phycoerythrin alpha chain, <i>Porphyra purpurea</i>	PHEA_PORPU	SVITTTISAADAAGR	717.3834	1134.5749 1033.5273 374.2146
		FPSSSDLESVQGNIQR	588.6235	715.3846 621.2515 587.3260
		NPGEAGDSQEK	566.2493	920.3956 663.2944 491.2460
C-phycoyanin-1 alpha chain, <i>Synechococcus</i> sp.	PHCA1_SYNP6	TPLTEAVAAADSQGR	743.8784	1175.5651 945.4748 775.3693
		FLSSTELQVAFGR	727.8855	1194.6113 1107.5793 790.457
C-phycoerythrin alpha chain, <i>Synechocystis</i> sp.	PHEA_SYNY1	TLGLPTAPYVEALSFR	602.6647	1152.6048 793.4203 664.3777
		FPSTSDLESVQGSIQR	584.2917	688.3737 635.2671 560.3151
C-phycoerythrin alpha chain, <i>Microchaete diplosiphon</i>	PHEA_MICDP	SVVTTVIAAADAAGR	701.3834	1116.6008 815.437 374.2146
		ALGLPTAPYVEALSFR	592.6612	1152.6048 793.4203 664.3777
		FPSTSDLESVQGSIQR	584.2917	688.3737 635.2671 560.3151

**Table 5**

Total spectrum, peptide and protein counts after purification by our approach versus published protocols on complex matrices.

	Total spectrum count	Peptide count	Protein count
Biofilm-published approach <sup>a</sup>	932	585	195
Biofilm-our approach <sup>a</sup>	937	424	163
Mouse liver-published approach <sup>a</sup>	1122	1408	416
Mouse liver-our approach <sup>a</sup>	959	1205	355
Soil-published approach <sup>b</sup>	946	293	72
Soil-our approach <sup>b</sup>	932	488	128

Data from the ProteomeXchange Consortium via the PRIDE [10] repository with the dataset identifier PXD0081110 and 10.6019/PXD0081110.

<sup>a</sup> Average of three replicates.<sup>b</sup> Counts of a single replicate.

## 2. Experimental design, materials and methods

Experimental design and materials and methods have been reported previously [1].

## Acknowledgments

This research was carried out with the financial support of the French Ministère de l'Enseignement Supérieur et de la Recherche (5HU66) and the Ligue contre le Cancer (Maj 06-12-2016)

## References

- [1] B. Eddhif, J. Lange, N. Guignard, Y. Batonneau, S. Papot, C. Geffroy-Rodier, P. Poinot, Study of a novel agent for TCA precipitated proteins washing - comprehensive insights into the role of ethanol/HCl on molten globule state by multi-spectroscopic analyses, *J. Proteomics*. 173 (2018) 77–88 (submitted for publication).
- [2] K. Chourey, J. Jansson, N. VerBerkmoes, M. Shah, K.L. Chavarria, L.M. Tom, E.L. Brodie, R.L. Hettich, Direct cellular lysis/protein extraction protocol for soil metaproteomics, *J. Proteome. Res.* 9 (2010) 6615–6622. <http://dx.doi.org/10.1021/pr100787q>.
- [3] H.-J. Huang, W.-Y. Chen, J.-H. Wu, Total protein extraction for metaproteomics analysis of methane producing biofilm: the effects of detergents, *Int. J. Mol. Sci.* 15 (2014) 10169–10184. <http://dx.doi.org/10.3390/ijms150610169>.
- [4] S. Song, G.J. Hooiveld, W. Zhang, M. Li, F. Zhao, J. Zhu, X. Xu, M. Muller, C. Li, G. Zhou, Comparative proteomics provides insights into metabolic responses in rat liver to isolated soy and meat proteins, *J. Proteome Res.* 15 (2016) 1135–1142. <http://dx.doi.org/10.1021/acs.jproteome.5b00922>.
- [5] L. Jiang, L. He, M. Fountoulakis, Comparison of protein precipitation methods for sample preparation prior to proteomic analysis, *J. Chromatogr. A*. 1023 (2004) 317–320. <http://dx.doi.org/10.1016/j.chroma.2003.10.029>.
- [6] E. Fic, S. Kedracka-Krok, U. Jankowska, A. Pirog, M. Dziedzicka-Wasylewska, Comparison of protein precipitation methods for various rat brain structures prior to proteomic analysis, *Electrophoresis*. 31 (2010) 3573–3579.
- [7] D.I. Jacobs, M.S. van Rijssen, R. van der Heijden, R. Verpoorte, Sequential solubilization of proteins precipitated with trichloroacetic acid in acetone from cultured *Catharanthus roseus* cells yields 52% more spots after two-dimensional electrophoresis, *Proteomics* 1 (2001) 1345–1350. [http://dx.doi.org/10.1002/1615-9861\(200111\)1:11 < 1345::AID-PROT1345 > 3.0.CO;2-F](http://dx.doi.org/10.1002/1615-9861(200111)1:11 < 1345::AID-PROT1345 > 3.0.CO;2-F).
- [8] A. Rygula, K. Majzner, K.M. Marzec, A. Kaczor, M. Pilarczyk, M. Baranska, Raman spectroscopy of proteins: a review: raman spectroscopy of proteins, *J. Raman Spectrosc.* 44 (2013) 1061–1076. <http://dx.doi.org/10.1002/jrs.4335>.
- [9] J.A. Vizcaino, A. Csordas, N. del-Toro, J.A. Dianes, J. Griss, I. Lavidas, G. Mayer, Y. Perez-Riverol, F. Reisinger, T. Ternent, Q. W. Xu, R. Wang, H. Hermjakob, 2016 update of the PRIDE database and related tools, *Nucleic Acids Res* 44 (2016) D447–D456. <http://dx.doi.org/10.1093/nar/gkv1145>.